

Magnetic anisotropy of mesoscale-twinned Ni-Mn-Ga thin filmsV. A. Chernenko,^{1,2,*} V. A. Lvov,^{3,4} V. Golub,³ I. R. Aseguinolaza,¹ and J. M. Barandiarán¹¹*Universidad del País Vasco, Departamento Electricidad y Electronica, P.O. Box 644, Bilbao 48080, Spain*²*Ikerbasque, Basque Foundation for Science, Bilbao 48011, Spain*³*Institute of Magnetism, Vernadsky Str. 36-b, Kyiv 03142, Ukraine*⁴*Department of Radiophysics, Taras Shevchenko University, Kyiv 01601, Ukraine*

(Received 2 June 2011; revised manuscript received 14 July 2011; published 15 August 2011)

The ferromagnetic resonance data obtained for the twinned orthorhombic martensitic phase of Ni-Mn-Ga film epitaxially grown on MgO(100) substrate are presented. The reported data prove that the mesoscale twinning reduces the value of in-plane magnetic anisotropy field of the Ni-Mn-Ga film by an order of magnitude. The reduced magnetic anisotropy field corresponds to the tetragonal symmetry, while the unit cells of the film are orthorhombic. The experimentally observed change of the in-plane magnetic anisotropy is explained in the framework of the magnetoelastic model of martensite, and the second-order and fourth-order magnetic anisotropy constants are evaluated. The perpendicular magnetic anisotropy constant proved to be negative and small in the absolute value. Therefore the estimated value of the magnetic domain wall width is comparable with the widths of mesoscale twins observed in the investigated film. This confirms an idea that the magnetic vectors of twin components are strongly coupled by the exchange interaction.

DOI: [10.1103/PhysRevB.84.054450](https://doi.org/10.1103/PhysRevB.84.054450)

PACS number(s): 75.50.Cc, 81.15.Cd, 76.50.+g, 75.70.Ak

I. INTRODUCTION

The Ni-Mn-Ga ferromagnetic shape memory alloys (FSMAs) are widely studied now (see e.g. overviews of Refs. 1–3 and references therein). The most attractive physical property of these alloys is a large ($\sim 10\%$) magnetic-field-induced strain (MFIS).^{1,2,4,5} The MFIS is caused by a rearrangement of the twin structure of the Ni-Mn-Ga single crystal under the magnetic field. This rearrangement, in its turn, is driven by the rotation of the magnetic moments of atoms. The twin boundary movement process starts when the magnetic field value^{4,5} and rotation angle⁶ reach certain threshold values.

Until recently, a strong magnetocrystalline anisotropy was considered as a feature inalienable from the FSMAs exhibiting MFIS.^{4,5} However, the stronger the magnetocrystalline anisotropy of the specimen, the higher the threshold magnetic field that is needed to rotate the magnetic moments noticeably and to initiate the movements of twin interfaces. Generally, a reduction of the threshold magnetic field value is a challenging scientific problem. Possible solutions of this problem have been proposed.^{7,8} Among them, a reduction of the effective magnetic anisotropy due to the micro- and mesoscale twinning of the crystal was considered.⁸

Whereas a simple theoretical model describing the influence of twinning on the magnetic anisotropy of FSMA was proposed some time ago,⁹ a direct experimental observation of the related physical effect has been realized recently.¹⁰ It was shown that the detwinning of twinned Ni-Mn-Ga crystal results in the noticeable change of magnetization curves.¹⁰ These curves indicate immediately that the detwinning reduces the magnetic susceptibility of the crystal. It may be concluded, therefore, that the disappearance of twins reinforces the effective magnetic anisotropy.

The magnetic anisotropy of Ni-Mn-Ga films was studied in Refs. 11–13 using the ferromagnetic resonance (FMR) technique. Commonly, the magnetic anisotropy energy density (MAED) of the films is smaller than the MAED of the bulk single crystals.^{11,12} As so, we undertook a special study

aimed at the direct experimental observation and theoretical interpretation of the influence of mesoscale twinning on the magnetic anisotropy of the representative Ni-Mn-Ga thin film.

In Sec. II, we report the FMR data obtained for the twinned Ni-Mn-Ga film exhibiting the orthorhombic martensitic structure. The reported data prove that the mesoscale twinning reduces the value of in-plane magnetic anisotropy field by an order of magnitude. The reduced in-plane magnetic anisotropy field corresponds to the tetragonal symmetry, implying that the fourfold symmetry axis is aligned along the film normal, while the unit cells of the film are orthorhombic.

Section III is devoted to the theoretical analysis of the experimental data. In this section, the experimentally observed change of the in-plane magnetic anisotropy is explained and the second-order and fourth-order magnetic anisotropy constants are evaluated.

In Sec. IV, we argue that the magnetic moments of twin components are strongly coupled by the spin-exchange interaction, and therefore, the twin structure may be considered as an ensemble of coupled magnetic moments, which oscillate in the effective magnetic field. The effective field is a superposition of the external field and the average anisotropy field, which is inherent to the twin structure as a whole.

II. EXPERIMENTAL RESULTS

The 0.5- μm -thick film of $\text{Ni}_{52.3}\text{Mn}_{26.8}\text{Ga}_{20.9}$ (at.%) epitaxially grown on heated MgO(001) substrate at 2.6×10^{-2} mbar pressure and 150 W power has been fabricated by magnetron sputtering. The FMR data were collected using the ELEXYS E500 Bruker EPR spectrometer (X-band, $\omega/2\pi = 9.46$ GHz) operating in the temperature range 100–450 K and equipped with an automatic goniometer. The value of the g factor derived from paramagnetic resonance measurements in austenitic state (above 420 K) proved to be close to 2.01. Composition of the film was determined with an accuracy better than 0.5 at.% by energy-dispersive x-ray spectroscopy (EDX), using a scanning electron microscope (SEM) Jeol JSM-6400.

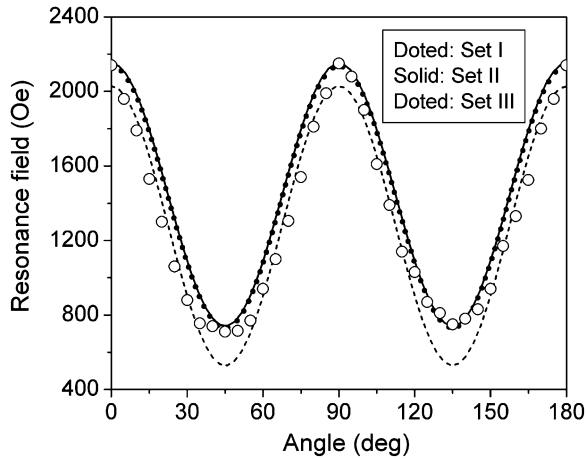


FIG. 1. Experimental angular dependence of the in-plane resonance field (open circles) in comparison with theoretical dependencies that were computed for the Set I (dots) and Set II (solid line) of physical values. The dashed line is computed for the Set I with the lattice parameter b adopted from the Set II. The line corresponding to the Set III is not shown because it is practically confluent with the solid line.

An SEM was also used for the microstructure observations in the secondary electron mode. The structural state of the film and its temperature variation was controlled by x-ray diffraction (Philips X'Pert PRO), using $\text{CuK}\alpha$ radiation. The cubic-to-orthorhombic martensitic transformation (MT) was observed at about 420 K.

The experimental angular dependence of the in-plane resonance field $H_r(\varphi)$ at 290 K is shown by the open circles in Fig. 1. Zero angle ($\varphi = 0$) corresponds to the [100] direction of the MgO substrate. The experimental angular dependence of the resonance field (open circles in Fig. 1) exhibits the fourfold symmetry in the film plane. The minima of the resonance field correspond to the magnetization easy directions, $\varphi = \pi/4 + \pi n/2$, $n = 0, 1, 2, \dots$. The out-of-plane angular dependence $H_r(\theta)$ (not shown in Fig. 1) is symmetrical with respect to the film normal, indicating its coincidence with the fourfold symmetry axis.

To follow the temperature evolution of magnetic parameters, the magnetic field was oriented normally to the film plane, and a temperature dependence of the resonance field value was measured (see Fig. 2). Due to the presence of the uniaxial magnetocrystalline anisotropy and magnetostatic field, the resonance values of the out-of-plane magnetic field substantially exceed the values obtained for the in-plane field orientation [see Sec. III, Eqs. (16) and (17)]. It is important that the resonance field monotonously decreases with the temperature increasing. Such a behavior is essentially different from the one which was observed previously in the tetragonal martensitic phase of Ni-Mn-Ga films with $c < a$, where the effective magnetization was decreasing during cooling as a result of the increasing of the out-of-plane anisotropy.^{13,14} This behavior suggests that the perpendicular anisotropy constant in the investigated film is either small or negative, in agreement with the FMR and data from a superconducting quantum interference device (SQUID) that confirm a formation of in-plane anisotropy and negative value of the perpendicular anisotropy constant.

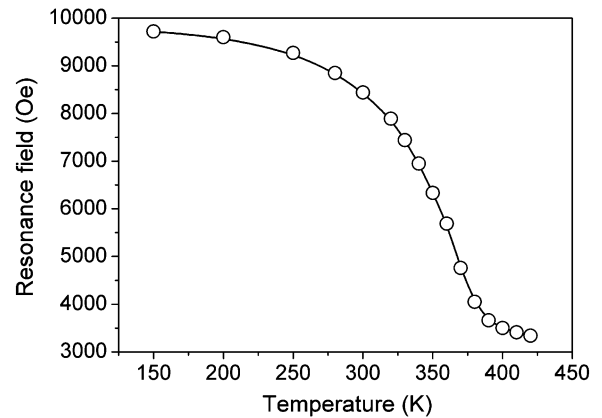


FIG. 2. Experimental temperature dependence of the resonance field value. Magnetic field vector was applied normally to the film plane.

Above 370 K, the resonance field rapidly drops, manifesting an approach to Curie point. It correlates with the magnetization data. However, even in the paramagnetic state, there is a difference in the resonance field values observed in the in-plane and perpendicular-to-the-plane configurations. This difference is usually described in terms of g -factor anisotropy, which is present at both sides of the martensitic transformation temperature (~ 420 K).

In the martensitic state, the film has a regular twin microstructure (Fig. 3), while the x-ray analysis shows a formation of orthorhombic crystal structure with the longest, a , and shortest, c , axes lying in the film plane, while b is perpendicular to the film plane. The x-ray, SEM, and FMR data give rise to the schematic in Fig. 4, where the crossing-twin-boundary structure (see e.g. Refs. 15 and 16) of twinned film, its magnetic domain structure, and twin-boundary orientations towards substrate are modeled. The inclinations of twin boundaries (45°) towards substrate and magnetic domain pattern are equivalent for both the rear and the front part of the drawing.

The SEM image shows the formation of fine twin structure with the characteristic twin width of about several tens of nanometers (Fig. 3). Similar twinning morphology has been observed in Refs. 17–20. For the twin structure shown in Figs. 3 and 4, two resonance peaks would be expected. The in-plane

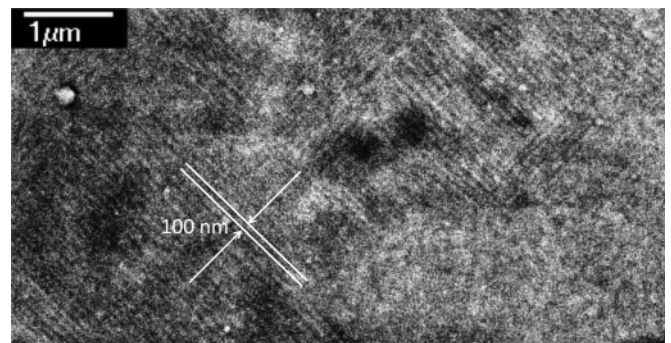


FIG. 3. Secondary electron image of the film surface revealing fine twinning in the orthorhombic martensite and its orientation with regard to a substrate. The twinning period is indicated.

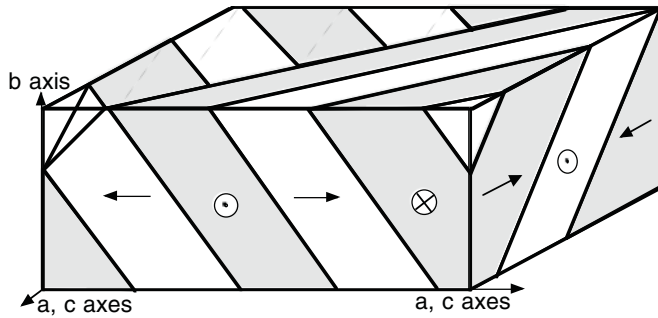


FIG. 4. The reconstructed from the x-ray diffraction data and SEM image (Fig. 3) schematic of the two-variant twin structure of Ni-Mn-Ga film, which consists of in-plane ac twin variants representing also 90° magnetic domains with the in-plane magnetization vectors aligned along easy c axis (arrows). The rear part of the drawing represents a set of variants, oriented at 90° from the front set with the same magnetic moments pattern as indicated in the front part. The direction of magnetization of the twins in the rear part of the drawing is similar to the front part. The a and c axes are parallel to the $\langle 110 \rangle_{\text{MgO}}$ directions.

angular dependencies of the corresponding resonance fields would be periodic with the period of 180° and would be shifted at 90° with respect to each other. Instead, only one resonance peak was observed in our experiments, and its in-plane angular dependence clearly shows the 90° periodicity. The apparent contradiction between the FMR and structural data can be resolved taking into account the exchange coupling of the magnetic moments of the twin components (see below).

It is worth noting that the FMR signal obtained at temperatures below 340 K is typical for the systems with gradually varying magnetic parameters. This variation results in the dispersion of the resonance field values. The dispersion can be characterized by the parameter ΔH_p (see Fig. 5). The variation of the experimental values of ΔH_p with the temperature is shown in Fig. 6. The $\Delta H_p(T)$ curve may be conventionally divided into two parts. Below 340 K, the resonance field dispersion decreases almost linearly with the temperature

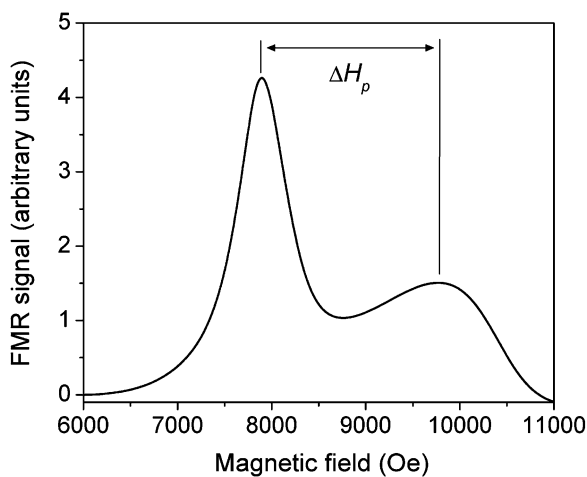


FIG. 5. Ferromagnetic resonance signal obtained at 320 K. Magnetic field is perpendicular to the film plane. The two-side arrow shows the average value of the resonance field dispersion.

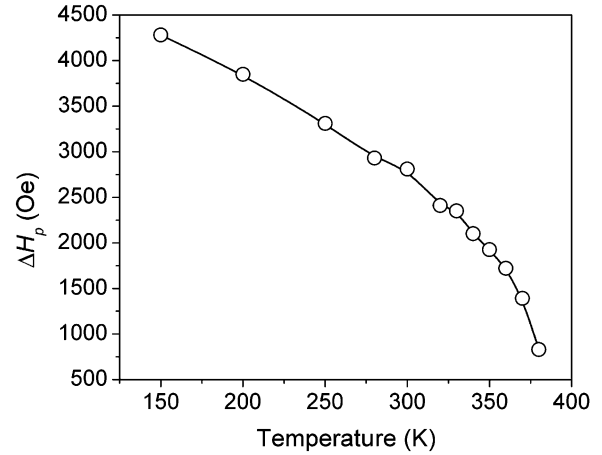


FIG. 6. Temperature dependence of a dispersion of the perpendicular resonance field.

increase. Above 340 K, a rapid drop of the ΔH_p value is observed.

III. EVALUATION OF MAED OF TWINNED Ni-Mn-Ga FILM

A. Formalism

The experimental FMR data obtained in the in-plane magnetic field show that the resonance conditions are prescribed by the MAED that is a periodic function of the angle between $[100]$ crystallographic direction and magnetic field. The period of variation of the resonance field value is equal to 90° . This periodicity is inherent to the periodic martensitic structure presented in Fig. 4, while the MAED of single-variant martensitic state must be periodic with the period of 180° . It suggests an idea that the resonance frequency/field values are prescribed by the average MAED of the martensitic structure formed by the alternating domains/variants of orthorhombic crystal lattice. In this case, the resonance oscillations of atomic spins are spatially uniform, and the spin exchange energy is constant. Thus, the angular dependence of the resonance field values can be described using the magnetoelastic model proposed in Ref. 9.

Let the coordinate system be related to $\langle 100 \rangle$ crystallographic directions. The martensitic structure presented in Fig. 4 consists of the crystallographic domains (martensite variants) with $a \parallel x$, $b \parallel z$ and $c \parallel x$, $b \parallel z$. Pairs of these variants form the twinned fragments of the film as it is evident in Fig. 3. The average MAED of the ac twin structure formed by the c and a variants is

$$\bar{F}_A(\alpha) = \alpha F_A^{(c)} + (1 - \alpha) F_A^{(a)}, \quad (1)$$

where α is a volume fraction $V_c/(V_a + V_c)$ of the c component in the twin structure, and $F_A^{(c)}$ and $F_A^{(a)}$ are the MAEDs of the twin components. The expressions for these MAEDs can be expanded in series with respect to the components of the magnetic vector. According to the first-principle computations²¹ and magnetoelastic model,⁹ the coefficients at the second-order terms of MAEDs of the twin components are proportional to the spontaneous deformation of the cubic lattice during the MT. The cubic-orthorhombic MT is

characterized by the diagonal strain tensor components that are expressed as

$$\varepsilon_{xx}^{(a)} = (a - a_0)/a_0, \quad \varepsilon_{yy}^{(a)} = (c - a_0)/a_0, \quad \varepsilon_{zz}^{(a)} = (b - a_0)/a_0 \quad (2)$$

for the a component and

$$\varepsilon_{xx}^{(c)} = (c - a_0)/a_0, \quad \varepsilon_{yy}^{(c)} = (c - a_0)/a_0, \quad \varepsilon_{zz}^{(c)} = (b - a_0)/a_0 \quad (3)$$

for the c component of the twin. (Here, a_0 is the value of lattice parameter in the cubic phase).

The second-order terms of MAEDs of the twin components are related to the MT strains as

$$F_{A2}^{(a,c)} = -\delta M^2 \left\{ \sqrt{3} u_2^{(a,c)} \left[(m_x^{(a,c)})^2 - (m_y^{(a,c)})^2 \right] + u_3^{(a,c)} \left[2(m_z^{(a,c)})^2 - (m_y^{(a,c)})^2 - (m_x^{(a,c)})^2 \right] \right\}, \quad (4)$$

where δ is a dimensionless magnetoelastic constant, $\mathbf{m}^{(a,c)} = \mathbf{M}^{(a,c)}/M$ is a unit magnetic vector of the a - or c -twin component, $\mathbf{M}^{(a,c)}$ is a magnetization vector of corresponding twin component, $M = |\mathbf{M}^{(a,c)}|$ (Ref. 9). The values $u_2^{(a,c)}$ and $u_3^{(a,c)}$ are the linear combinations of MT strains expressed as

$$u_2^{(a,c)} = \sqrt{3} (\varepsilon_{xx}^{(a,b)} - \varepsilon_{yy}^{(a,b)}), \quad u_3^{(a,c)} = 2\varepsilon_{zz}^{(a,c)} - \varepsilon_{yy}^{(a,c)} - \varepsilon_{xx}^{(a,c)}. \quad (5)$$

The maximum possible effect of a fine twinning on the magnetic anisotropy of the ferromagnetic single crystal can be derived under the assumption that the magnetic vectors of the neighboring twin components are strongly coupled by the spin exchange interaction. In this case, the twin structure is characterized by the single magnetic vector $\mathbf{m} = \mathbf{M}/M$,²² and the equilibrium direction of this vector is prescribed by the average MAED of the twinned orthorhombic lattice.^{8,9} As far as the MAED of ferromagnetic martensite depends linearly on the strain tensor components, an averaging of MAEDs is equivalent to the averaging of MT strains. The average MT strains are characterized by the strain tensor components

$$\bar{\varepsilon}_{ii}^{(ac)} = \alpha \varepsilon_{ii}^{(c)} + (1 - \alpha) \varepsilon_{ii}^{(a)}. \quad (6)$$

A substitution of the MT strains expressed by the Eqs. (2) and (3) into the Eqs. (4)–(6) yields the simple formula

$$\bar{F}_{A2}(\alpha) = K_{\perp} m_z^2 + (1 - 2\alpha) K_{\parallel} (m_x^2 - m_y^2), \quad (7)$$

where

$$K_{\parallel} = -3\delta M^2 (a - c)/a_0, \quad (8)$$

$$K_{\perp} = -3\delta M^2 (2b - a - c)/a_0$$

are the second-order magnetic anisotropy constants that are inherent to the single-variant martensitic state.

The fourth-order terms of MAEDs of the twin components are expressed as

$$F_{A4}^{(a)} = -\frac{1}{2} (K_a m_x^4 + K_c m_y^4 + K_b m_z^4), \quad (9)$$

$$F_{A4}^{(c)} = -\frac{1}{2} (K_c m_x^4 + K_a m_y^4 + K_b m_z^4),$$

where K_a , K_b , and K_c are the fourth-order anisotropy constants. According to the Eq. (1), the fourth-order terms in the expression for the average MAED have the form

$$\bar{F}_{A4}(\alpha) = -\frac{1}{2} [K_{ca}(\alpha) m_x^4 + K_{ca}(1 - \alpha) m_y^4 + K_b m_z^4], \quad (10)$$

where

$$K_{ca}(\alpha) = \alpha K_c + (1 - \alpha) K_a, \quad (11)$$

$$K_{ca}(1 - \alpha) = (1 - \alpha) K_c + \alpha K_a.$$

Let the external magnetic field be applied along the i -axis. The magnetic energy density is

$$\bar{F}(\alpha) = \bar{F}_{A2}(\alpha) + \bar{F}_{A4}(\alpha) + 2\pi M^2 m_z^2 - m_i H_i M. \quad (12)$$

The sum of the first and second terms on the right side of Eq. (12) is the average MAED expressed by Eq. (1); the third and fourth terms are the magnetostatic and Zeeman energy densities, respectively. If the external magnetic field is equal to zero, the energy difference between the states with $\mathbf{m} \parallel x$ and $\mathbf{m} \parallel y$ is equal to

$$\bar{F}_{\mathbf{m} \parallel x}(\alpha) - \bar{F}_{\mathbf{m} \parallel y}(\alpha) = \frac{1}{2} (1 - 2\alpha) (4K_{\parallel} + K_c - K_a). \quad (13)$$

For the Ni-Mn-Ga martensites, the inequalities $4K_{\parallel} > |K_c - K_a| > 0$ hold,⁸ and therefore, the easy magnetization direction (that is to say, the equilibrium direction of the magnetic vector) is parallel to the y axis if $\alpha < 1/2$ and to the x axis if $\alpha > 1/2$. In the case of $\alpha = 1/2$, the energy difference, Eq. (13), is equal to zero, and the equilibrium directions of the magnetic vector in the film plane correspond to the minimums of the fourth-order terms in the MAED.

Usually the dynamics of the unit magnetic vector are described by the equation

$$\frac{d\mathbf{m}}{dt} = \gamma (\mathbf{m} \times \bar{\mathbf{H}}^{\text{eff}}), \quad (14)$$

where $\bar{\mathbf{H}}^{\text{eff}} = -M^{-1} (\partial \bar{F} / \partial \mathbf{m})$ is the average value of the effective magnetic field acting on the magnetic vector. When a magnetic field is applied in the film plane, the energy, Eq. (14), corresponds to the resonance field values, which satisfy the equation

$$\frac{\omega^2}{\gamma^2} = (\bar{H}_{0x}^{\text{eff}})^2 + (\bar{H}_{0y}^{\text{eff}})^2 - \bar{H}_{0x}^{\text{eff}} (\bar{H}_z^{\text{eff}} + \bar{H}_{1y}^{\text{eff}}) \times \cos \varphi - \bar{H}_{0y}^{\text{eff}} (\bar{H}_z^{\text{eff}} + \bar{H}_{1x}^{\text{eff}}) \sin \varphi + \bar{H}_z^{\text{eff}} (\bar{H}_{1x}^{\text{eff}} \sin^2 \varphi + \bar{H}_{1y}^{\text{eff}} \cos^2 \varphi), \quad (15)$$

where

$$\bar{H}_{0x}^{\text{eff}} = H_x + 2M^{-1} [(2\alpha - 1)K_{\parallel} + K_{ca}(\alpha) \cos^2 \varphi] \cos \varphi,$$

$$\bar{H}_{0y}^{\text{eff}} = H_y + 2M^{-1} [(1 - 2\alpha)K_{\parallel} + K_{ca}(1 - \alpha) \sin^2 \varphi] \sin \varphi,$$

$$\bar{H}_{1x}^{\text{eff}} = 2M^{-1} [(2\alpha - 1)K_{\parallel} + 3K_{ca}(\alpha) \cos^2 \varphi],$$

$$\bar{H}_{1y}^{\text{eff}} = 2M^{-1} [(1 - 2\alpha)K_{\parallel} + 3K_{ca}(1 - \alpha) \sin^2 \varphi],$$

$$\bar{H}_z^{\text{eff}} = -2K_{\perp} M^{-1} - 4\pi M$$

are the average values of the effective magnetic field components, and φ is the angle between the unit magnetic vector and the $[100]$ direction.

Now, let the magnetic field be applied normally to the film plane. For the theoretical interpretation of the experimental results, we will consider the most instructive cases $\alpha = 0$ (single variant martensitic state) and $\alpha = 1/2$ (the twinned martensite with the equal volume fractions of twin components). Taking into account the condition $m_x^2 + m_y^2 + m_z^2 = 1$, one can obtain the expression

$$\bar{F}(\alpha) = [K_2(\alpha) + 2\pi M^2]m_z^2 - \frac{1}{2}K_4(\alpha)m_z^4 - m_z H_z M, \quad (16)$$

where for $\alpha = 0, 1/2$,

$$K_2(0) = K_{\perp} + K_{\parallel} + K_c,$$

$$K_4(0) = K_b + K_c,$$

$$K_2(1/2) = K_{\perp} + (K_a + K_c)/2,$$

$$K_4(1/2) = K_b + (K_a + K_c)/2.$$

The resonance value of transversal magnetic field satisfies the equation

$$H_r^{\perp}(\alpha) = \frac{\omega}{\gamma} + 4\pi M + \frac{2K_2(\alpha)}{M} - \frac{2K_4(\alpha)}{M}, \quad (17)$$

which shows that the twinning reduces the resonance field value and the reduction is equal to

$$H_r^{\perp}(0) - H_r^{\perp}(1/2) = \frac{2K_{\parallel}}{M}. \quad (18)$$

Eqs. (15), (17), and (18) enable a straightforward interpretation of the experimental results and a consistent evaluation of the second-order and fourth-order MAED constants of the film involved in Eqs. (7) and (9).

B. Computations

The resonance values of in-plane magnetic fields depend on the angle between the magnetic field and the [100] direction, in accordance with Eq. (15). If the field value satisfies the inequality $HM > K_a + K_c$, the field direction will be close to the direction of the magnetic vector, and therefore, the approximate values $H_x \approx H \cos\varphi$ and $H_y \approx H \sin\varphi$ can be substituted into Eq. (15). The last equation includes both second-order and fourth-order magnetic anisotropy constants. The second-order magnetic anisotropy constants, Eq. (8), are proportional to the magnetoelastic constant δ , the square of the magnetization value, and the linear combinations of the lattice parameters.

A computation of the periodic angular dependence of the in-plane resonance field $H_r^{\parallel}(\varphi)$ can be carried out using the value of $\alpha = 1/2$, the well-established value of the dimensionless magnetoelastic constant $\delta = -23$ (Refs. 6 and 7), and the experimental values of the lattice parameters. The magnetic anisotropy constants can be evaluated using the following fitting procedure:

(i) At the first step, the magnetization value must be adjusted to obtain the correct average value of the $H_r^{\parallel}(\varphi)$ function (the adjusted value proves to be independent on the values of the fourth-order anisotropy constants).

(ii) At the second step, the fourth-order anisotropy constant $2K_c a(1/2) = K_c + K_a$, which controls the amplitude of $H_r^{\parallel}(\varphi)$ function, should be adjusted to fit the plot of this function to

TABLE I. The physical values obtained by fitting procedure using the angular dependence of the in-plane resonance field and three sets of lattice parameters. See text for details.

	Set I	Set II	Set III
a , nm	0.612	0.612	0.619
b , nm	0.578	0.582	0.580
c , nm	0.554	0.554	0.553
M , emu/cm ³	590	495	610
$K_a + K_c$ (erg/cm ³)	-6×10^5	-5×10^5	-6.5×10^5
K_b (erg/cm ³)	8×10^5	4×10^5	9×10^5
K_{\parallel} (erg/cm ³)	2.41×10^6	1.68×10^6	2.92×10^6
K_{\perp} (erg/cm ³)	-4.16×10^5	-5.81×10^4	-5.31×10^5
$(K_a + K_c)/M$ (kOe)	-1.02	-1.01	-1.07
$2K_{\parallel}/M$ (kOe)	8.17	6.81	9.58
$2K_{\perp}/M$ (kOe)	-1.41	-0.235	-1.74
$H_r^{\perp}(1/2)$ (kOe)	8.74	8.68	8.69
$H_r^{\perp}(0)$ (kOe)	16.9	15.5	18.3

the experimental values of the resonance field (the amplitude proves to be independent on the K_b value).

(iii) Finally, the proper value of the K_b constant must be adjusted to fit the theoretical value of the transversal resonance field H_r^{\perp} to the experimental one.

We performed such a fitting procedure for three somewhat different sets of the lattice parameters to illustrate its high sensitivity to the variation of physical properties. During the procedure performance, the theoretical values of the resonance field were adjusted to the experimental ones at room temperature using $g = 2.01$.

The experimental values of lattice parameters reported in Ref. 23 and the adjusted values of the magnetization and anisotropy constants are presented in the Table I as the Set I of physical values. Corresponding to these values, the function $H_r^{\parallel}(\varphi)$ is presented in Fig. 1 by the dotted line.

Then the value $b = 0.578$ nm, reported in Ref. 23, was tentatively replaced by the value $b = 0.582$ nm, as determined in the present work, whereas the other values in the Set I were kept unchanged. The dashed line in Fig. 1 shows that this replacement resulted in the noticeable disagreement between the computed and experimental values of the resonance field. The divergence of the dotted and dashed lines illustrates a high sensitivity of the calculated values to the small variation of the physical properties, particularly to the lattice parameters. Thus, the fitting procedure was performed for the Set II of physical parameters, and the appropriate values of the anisotropy constants were determined (see Table I). The function $H_r^{\parallel}(\varphi)$, corresponding to these values, is presented in Fig. 1 by the solid line.

Finally, the fitting procedure was performed for the experimental values of the lattice parameters reported in Ref. 24. These values and the appropriate anisotropy constants are presented in Table I as the Set III. The corresponding function $H_r^{\parallel}(\varphi)$ is not presented in Fig. 1 because its plot almost coincides with the plot shown by the solid line.

For all sets of lattice parameters, the following conclusions can be derived:

(a) the in-plane anisotropy constant K_{\parallel} is positive, while the transversal anisotropy constant is negative;

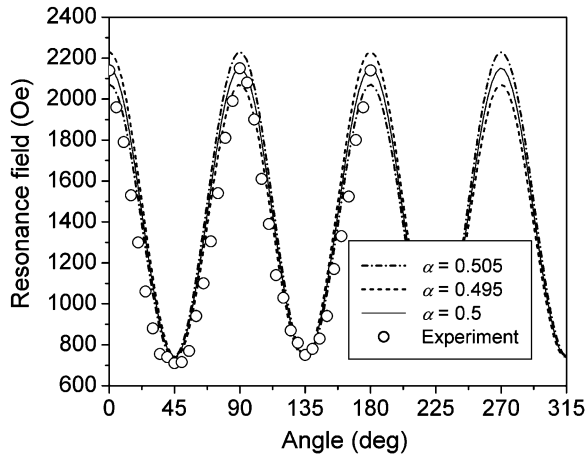


FIG. 7. The in-plane resonance field values computed for the complete (solid line) and partial (dashed and dash-dotted lines) compensation of the orthorhombic in-plane anisotropy of the film.

- (b) the inequality $K_{\parallel} \gg |K_{\perp}|$ holds;
- (c) the sum of the fourth-order anisotropy constants $K_c + K_a$ is negative, while K_b value is positive;
- (d) the absolute value of the fourth-order anisotropy field is smaller than the average magnitude of the resonance field but larger than the minimal value of this field. Therefore, the nonparallelism between the field vector and unit magnetic vector should be taken into account for the accurate computation of the $H_r(\varphi)$ function in the vicinity of its minimums.

Figure 7 illustrates the degree of perfection of the in-plane anisotropy compensation in the twinned film: the bifurcation of the $H_r(\varphi)$ function becomes noticeable even in the case of small deviation $\Delta\alpha = 0.05$ of the fractional parameter α from the value of $\alpha = 1/2$, which provides the perfect compensation of the orthorhombic in-plane anisotropy. This takes place because the strong inequality $K_{\parallel} \gg K_a + K_c$ is fulfilled. The experimental difference between the values $H_r(90)$ and $H_r(180)$ is substantially smaller than the theoretical one.

Twinning changes the FMR conditions also for the magnetic field perpendicular to the film plane. The computations carried out using Eq. (17) and Sets I–III of the physical parameters showed that the resonance field value $H_r^{\perp}(1/2)$, which is inherent to the twinned film, is nearly half of the value $H_r^{\perp}(0)$, which corresponds to the single-variant film. Thus, the twinning results in the considerable reduction of the perpendicular resonance field. It should be stressed that the second experimental value of the resonance field $H \approx 11.5$ kOe is considerably different from the theoretical values that were computed for the single-variant state of the film.

IV. DISCUSSION

The computed values of the magnetic anisotropy constants enable the estimation of the magnetic domain wall width l_0 . As

it is known, the width of the 90° domain wall can be roughly estimated from the formula $l_0 \sim a(H_E/H_A)^{1/2}/2$, where H_E and H_A are the internal magnetic fields that characterize the spin exchange interaction and the magnetocrystalline anisotropy, respectively. The value of $H_E \approx 9 \times 10^2$ kOe was reported for the Ni-Mn-Ga alloy.²⁵ For the Bloch domain wall, the characteristic anisotropy field is defined as $H_A = |2K_{\perp}|/M$, and therefore, the estimated values of the domain wall width are equal to 8, 19, and 7 nm for the Sets I, II, and III of the lattice parameters.

All estimated values of the magnetic domain wall width are comparable with the widths of twins, which are visible in Fig. 3. This confirms an idea that the components of twins are strongly coupled by the exchange interaction. The frequency of the homogeneous precession of the magnetic moments of atoms is predetermined by the average MAED, which is expressed by Eq. (16). The experimental values of the resonance field coincide with the theoretical ones computed for the parameter $\alpha = 1/2$ because they correspond to the resonance of the ensemble of twins, which means that $\alpha = 1/2$ is an average value being inherent to this ensemble. The homogeneous precession of the magnetic moments of the twin components is not accompanied by the variation of the local values of magnetization function $\mathbf{M}(\mathbf{r})$, and so it was described above by the precession of unit magnetic vector [see Eq. (14)].

The inhomogeneous oscillations of the magnetic moments of twin components result in the variation of the local values of the magnetization function $\mathbf{M}(\mathbf{r})$. As so, these oscillations are accompanied by the periodic variation of the spatial density of spin exchange interaction. Due to this, the resonance value of the transversal magnetic field coincides neither with the value of $H_r^{\perp}(1/2)$ that is inherent to the twinned film, nor with the magnitude of $H_r^{\perp}(0)$, which corresponds to the FMR in the single-variant film. As so, the exchange energy density $F_{ex}(\mathbf{r}) \propto [\nabla\mathbf{M}(\mathbf{r})]^2$ should be taken into account for the computation of the second resonance value of a transversal magnetic field. In essence, this energy density describes the exchange interaction between the spins of atoms situated in the neighboring twin components. This interaction prescribes the width of the magnetic domain walls and may contribute to the spatial dispersion of the spin waves propagating in the twinned magnetic film or the bulk single crystal. The role of the energy $F_{ex}(\mathbf{r})$ in the formation of the properties of fine-twinned magnetic films may be considered as a subject of the further theoretical work.

ACKNOWLEDGMENTS

The financial support from the Department of Education, Basque Government (Project ETORTEK No. IE10-272), the Spanish Ministry of Education and Science (Project No. MAT2008 06542-C04-02), and the Science and Technology Center in Ukraine (Project 5210) is acknowledged.

*volodymyr_chern@yahoo.com

¹R. C. O'Handley and S. M. Allen, in *Encyclopedia of Smart Materials*, edited by M. Schwartz (Wiley, New York 2002), p. 936.

²O. Söderberg, I. Aaltio, Y. Ge, X. W. Liu, and S. P. Hannula, *Adv. Sci. Tech.* **59**, 1 (2008).

³V. A. Chernenko and V. A. L'vov, *Mater. Sci. Forum* **583**, 1 (2008).

- ⁴S. J. Murray, M. Marioni, S. M. Allen, and R. C. O'Handley, *Appl. Phys. Lett.* **77**, 886 (2000).
- ⁵A. Likhachev, A. Sozinov, and K. Ullakko, *Mat. Sci. Eng. A* **378**, 513 (2004).
- ⁶C. P. Sasso, V. A. Lvov, V. A. Chernenko, J. M. Barandiaran, M. Pasquale, and Y. Kono, *Phys. Rev. B* **81**, 224428 (2010).
- ⁷V. Chernenko, V. L'vov, E. Cesary, J. Pons, R. Portier, and S. Zagorodnyuk, *Mat. Trans. JIM* **43**, 856 (2002).
- ⁸V. A. Lvov and V. A. Chernenko, *Mat. Sci. Forum* **684**, 31 (2011).
- ⁹V. A. Lvov, E. V. Gomonaj, and V. A. Chernenko, *J. Phys. Condens. Mat.* **10**, 4587 (1998).
- ¹⁰O. Heczko, L. Straka, V. Novak, and S. Fähler, *J. Appl. Phys.* **107**, 09A914 (2010).
- ¹¹J. Dubowik, Y. V. Kudryavtsev, and Y. P. Lee, *J. Appl. Phys.* **95**, 2912 (2004).
- ¹²B. D. Shanina, A. A. Konchits, S. P. Kolesnik, V. G. Gavriljuk, I. N. Glavatskij, N. I. Glavatska, O. Söderberg, V. K. Lindroos, and J. Foct, *JMMM* **237**, 309 (2001).
- ¹³V. A. Chernenko, V. Golub, J. M. Barandiaran, O. Y. Salyuk, F. Albertini, L. Righi, S. Fabbrici, and M. Ohtsuka, *Appl. Phys. Lett.* **96**, 042502 (2010).
- ¹⁴V. Golub, K. M. Reddy, V. Chernenko, P. Müllner, A. Punnoose, and M. Ohtsuka, *J. Appl. Phys.* **105**, 07A942 (2009).
- ¹⁵J. Z. Liu, Y. X. Jia, R. N. Shelton, and M. J. Fluss, *Phys. Rev. Lett.* **66**, 1354 (1991).
- ¹⁶P. Müllner, V. A. Chernenko, and G. Kostorz, *J. Appl. Phys.* **95**, 1531 (2004).
- ¹⁷M. Thomas, O. Heczko, J. Buschbeck, U. K. Röbber, J. McCord, N. Scheerbaum, L. Schultz, and S. Fähler, *New J. Phys.* **10**, 023040 (2008).
- ¹⁸M. Thomas, O. Heczko, J. Buschbeck, L. Schultz, and S. Fähler, *Appl. Phys. Lett.* **92**, 192515 (2008).
- ¹⁹J. Tillier, D. Bourgault, S. Pairisa, L. Ortega, N. Caillault, and L. Carbone, *Physics Procedia* **10**, 168 (2010).
- ²⁰G. Jakob, T. Eichhorn, M. Kallmayer, and H. J. Elmers, *Phys. Rev. B* **76**, 174407 (2007).
- ²¹J. Enkovaara, A. Ayuela, L. Nordström, and R. M. Nieminen, *Phys. Rev. B* **65**, 134422 (2002).
- ²²K. Y. Guslienko, N. A. Lesnik, A. I. Mitsek, and B. P. Vozniuk, *J. Appl. Phys.* **69**, 5316 (1991).
- ²³V. V. Martynov and V. V. Kokorin, *J. de Phys. III* **2**, 739 (1992).
- ²⁴A. Sozinov, A. Likhachev, and K. Ullakko, *IEEE Trans. Mag.* **38**, 2814 (2002).
- ²⁵V. A. Chernenko, V.A. L'vov, E. Cesari, and P. McCormick, *Mater. Trans. JIM* **41**, 928 (2000).